J Mater Sci: Mater Med (2008) 19:929–936
DOI 10.1007/s10856-007-3016-7

Fracture strength and adhesive strength of hydroxyapatite-filled polycaprolactone

Shing-Chung Wong · Avinash Baji

Received: 16 March 2006 / Accepted: 27 March 2007 / Published online: 1 August 2007

Abstract Fracture toughness and tear strength of hydroxyapatite (HAP)-filled poly(ε-caprolactone) (PCL) with increasing HAP concentration were studied. The toughness was assessed in terms of essential work of fracture (EWF). Adhesive strength between HAP and PCL interfaces was evaluated using T-peel testing. The adhesion between the two components was found to be relatively strong. Double edge notched tension (DENT) and trousers test specimens were used for the EWF tests. The effect of HAP phase in PCL on the fracture and tearing toughness was investigated. The results obtained from the EWF tests for the HAP-filled PCL complied with the validity criteria of the EWF concept, namely, (1) geometric similarity for all ligament lengths; (2) fully yielded ligament and (3) plane-stress fracture condition. Values for specific essential work of fracture (w_e) and specific plastic work of fracture (βw_p) were found to decrease with increase in HAP concentration. The testing procedure showed promise in quantifying the tearing resistance and rising *R*-curve behavior common in natural materials and it can be extended to other biomaterials that exhibit post-yield deformation. A quantitative assessment based on fracture mechanics of the adhesive strength between the bioactive interfaces plays an important role for continued development of tissue replacement and tissue regeneration materials.

S.-C. Wong (✉) · A. Baji
Department of Mechanical Engineering, The University of Akron, Akron, OH 44325-3903, USA
e-mail: swong@uakron.edu

Introduction

Biodegradable polymers reinforced by bioactive ceramics such as hydroxyapatite (HAP) have been widely studied for potential applications in tissue engineering [1–4]. An in-depth understanding of bioactive composites [3] offers attractive potential for tissue replacement and tissue regeneration. Most efforts concentrated on processing routes for tissue scaffolds such as fused deposition [5, 6], computer-aided manufacturing [7, 8] and other freeform fabrication techniques [9, 10]. Little is understood on how to design tough and strong scaffolds that emulate interactively the mechanical behavior of human bones. All scaffolds need to be mechanically robust like bones, yet many are weak and brittle, fracturing under impact or cyclic fatigue loading easily. Studies on toughness characterization of cortical [11–15] bones were done in the last few decades but the high toughness values of natural materials (bovine femoral cortical bone: longitudinal K_{Ic} ~ 3.2 MPa$\sqrt{m}$ [11] and transverse K_{Ic} ~ 6.56 MPa$\sqrt{m}$ [12], human cortical bone K_c ~ 2 MPa$\sqrt{m}$ [14]) were not obtained from biomimetic equivalents (monolithic HAP ~ 0.6 MPa$\sqrt{m}$ and HAP/nylon ~ 0.8 MPa$\sqrt{m}$ [16]). Natural bones show a rising *R*-curve behavior, K_R, which suggests toughening mechanisms operate in the crack wake as cracks propagate. Most tissue engineering studies on mechanical properties only characterize the tensile strength and stiffness [17–19], with little reference to fracture mechanics, which was widely employed for the study of natural and human bones [11–16]. It is important for researchers to gain an understanding of the micro/nano structures of natural materials and translate them into the design of bone analogue materials, or to optimize the properties of scaffold tissues via other materials design strategies. At present, an in-depth understanding of the design principles for tough

scaffolds that emulate natural species is lacking. This paper enables future comparative studies between bone analogue materials and natural bones and cartilage to be conducted on a mechanics basis.

Work of fracture measurements

In our laboratory, hydroxyapatite (HAP) filled poly(ε-caprolactone) (PCL) was evaluated for fracture toughness using the essential work of fracture (EWF) technique [20, 21]. The objective is to understand the parameters that govern the mechanics and mechanisms of fracture of such scaffolds as bone analogue materials [1–4]. The EWF technique was first developed to assess the toughness arising from the fracture process zone (FPZ) of metals by Cotterell and Reddell [20], followed by ductile thermoplastics [21–24]. The FPZ is assumed to be embedded in a large specimen and allowed to fully develop with complete yielding prior to crack propagation. The essential work is to include the essential elastic and plastic energies required for developing the FPZ that can be accommodated by the specimen size. Under strict conditions, the specific essential work of fracture is a material property independent of specimen geometry and only dependent on the specimen thickness. It is a unique method to characterize the fracture toughness of thin and ductile materials samples. In quasi-static crack growth, the total fracture work, W_f, can be partitioned into two components: (i) the essential work performed in the FPZ, W_e, and (ii) non-essential work performed in the outer plastic zone, W_p. When both the FPZ and the plastic zone are contained within the ligament, the essential work is proportional to the ligament size (l) but the non-essential work to the square of the ligament (l^2). Hence,

$$W_f = w_e l t + \beta w_p l^2 t \tag{1}$$

$$w_f = \frac{W_f}{lt} = w_e + \beta w_p l \tag{2}$$

where w_f is the specific total fracture work ($=W_f/lt$), β the geometry-dependent plastic zone shape factor, w_p the specific non-essential plastic work and t the thickness of the specimen. Plotting w_f against l yields a straight line, whose y-intercept gives w_e and whose slope equals βw_p. Equation 2 permits an extrapolated value, w_e, at zero ligament length (i.e. zero crack growth) and this value is the FPZ toughness of materials. This experimental approach provides a sound basis to determine w_e from work of fracture experiments using a range of ligament lengths and different specimen geometries [25, 26]. The physical meaning of w_e can be interpreted as follows. Consider a fully developed FPZ of length ρ_c and width d formed at the crack tip. The total fracture work dissipated in this process zone involves the work to cause necking and subsequent work necessary to draw out and eventually fracture the necked down material. The theoretical definition of w_e had been previously given [21, 22, 24] as:

$$w_e = d\int_0^{\bar{\varepsilon}_n} \bar{\sigma} d\bar{\varepsilon} + \int_{\varepsilon_n d}^{\delta_c} \sigma(\delta) d\delta \tag{3}$$

where $(\bar{\sigma}, \bar{\varepsilon})$ are true stress and true strain, $\bar{\varepsilon}_n$ and ε_n are true and engineering necking strains; δ is crack tip opening displacement within a characteristic FPZ and δ_c is the critical value at tearing. In this study, we report w_e obtained from double edge notched tension (DENT) and trousers test specimens of HAP-filled PCL.

The trousers test [21, 27–31] is an established technique to investigate the out-of-plane energy in tearing ductile materials. This test was introduced to evaluate the tear resistance of semicrystalline polymers and thin specimens [21, 27–31]. The specific essential work of fracture and non-essential specific plastic work can be determined from the tearing force [27–29]:

$$w_e = \frac{F}{t^2} = 2w_p t \tag{4}$$

where F is the equilibrium tearing force that is constant during steady state tearing of the specimen. A major difference between Eqs. 2 and 4 is the loading mode; Mode I for DENT and Mode III for trousers tearing. During trousers tearing of the specimen, the force usually rises until reaching an equilibrium level, where steady state tearing takes place, and falls on completion. It is well-known that the resistance to fracture under Mode I can be substantially enhanced by uniaxial orientation of molecules whereas the Mode III out-of-plane fracture involves the deformation of tie molecules which connect lamellar and fibrillar molecules, the mechanism of which promotes stress concentration and reduces microstructural response and fracture resistance.

Interfacial fracture toughness using peel tests

One practical factor in scaffold design is use of a strong and engineered interface between dispersed phases and the host matrix. Despite the lack of apparent chemical bonding, the HAP-PCL interface via mechanical interlock is of critical importance to successful development of scaffold materials using various computer-aided and freeform fabrication techniques. In this study, we examine the interfacial adhesion using a T-peel test [32–34]. The peel strength between adhering layers of HAP and PCL materials is measured to gain a better understanding of the interfacial work of fracture and its influence on the mechanical properties and overall fracture toughness. Peel strength

measures the force per unit width and as such is a measure of the input energy in conducting the peel and to separate the HAP-PCL interface. To the authors' knowledge, the interfacial work of fracture between HAP and PCL has not been previously studied in detail. This test is considered appropriate because there is little chemical interaction between HAP and PCL phases. The adhesion of dispersed HAP in PCL can be meaningfully quantified using peel laminates. The peel adhesion data can provide guidance for future correlation between the morphological design and interfacial adhesion.

Experimental work

Materials

The biodegradable polymer, polycaprolactone (PCL) (Molecular weight = 80,000) was from Sigma–Aldrich (Milwaukee, WI) and sintered hydroxyapatite (HAP) of particle size 53–124 μm was obtained from Clarkson Chromatography Products Inc. (South Williamsport, PA). PCL was dried under vacuum at 40 °C for 36–48 h. HAP was dry blended followed by extrusion using a Haake minilab twin screw extruder (Thermo Electron Corp., Hamburg, Germany) at 130 °C. Screw speed was 60 rpm and residence time was on average 6 min. Composites with 10, 20 and 30 wt% HAP were prepared. Rectangular bar (1.27 × 12.7 × 63.5 mm) and dog bone specimens (3.17 × 3.17 × 63.5 mm) were injection molded. These specimens were used for mechanical testing and toughness assessment. Specimens for peel tests were prepared independently using hot press. PCL-HAP-PCL flexible laminates were compression molded with a Teflon sheet separating part of the surfaces. Rectangular strips (1 × 18 × 126 mm) of PCL-HAP-PCL laminates were cut from the compression-molded piece to perform T-peel tests [34] as shown in Fig. 1. The peel arm length ~ 60 mm.

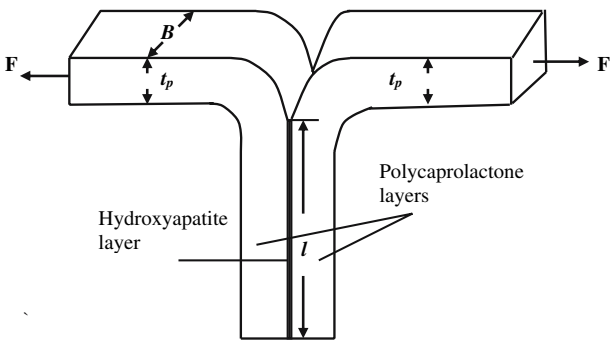

Fig. 1 T-peel test specimen. F represents the peel force, B and t_p represents the width and thickness of PCL layer. HAP layer is sandwiched between the two PCL layers

Mechanical properties

Tensile tests were performed at a crosshead speed of 10 mm/min using the dog bone specimens with an Instron 5582 test machine. An average of 5 specimens for each composition was tested. An extensometer was used to directly measure the tensile strain. Ultimate tensile strength and Young's modulus were assessed for all composites. Mean value and standard deviation were calculated for each group of composites. Analysis of variance (ANOVA) tests were performed to determine the statistical significance, indicated by the significance level $p < 0.05$, which suggests the trend of our data is statistically meaningful.

Rectangular double-edge-notched tension (DENT) specimens and trousers test specimens were used for the EWF tests. Specimens of width, B, and length, H, were tested. The dimensions of the DENT and trousers test specimens are shown in Figs. 2 and 3, respectively. Sharp notches were introduced into the specimen by using a fresh razor blade. The notches on the DENT specimens were created with equal lengths and directly opposite each other. The actual thickness of the specimen torn through was measured independently. Each specimen was loaded to complete failure. The load-deflection curves were recorded and the total energy to failure, W_f, was calculated for various ligament lengths. The specimens showed fully yielded ligaments.

Tear resistance of the composites was assessed using trousers tests. A crack of length, C, was cut along the axial direction of the specimen resulting in two legs of width, B_1 and B_2, using a sharp razor blade. Side grooves were made along the centerlines of trousers specimens to guide the crack propagation. The ends of the legs were clamped and pulled in opposite directions. The stress distribution in the specimen can be divided in regions shown in Fig. 3. Region X is the end region. Region Y represents the torn region. Region O is present only when the specimen is sufficiently large and it experiences uniaxial tension. Region Z is undeformed. Tear force was recorded against crosshead displacement.

Electron microscopy (SEM and TEM)

The specimens obtained from the mechanical tests were used for scanning electron microscopy (SEM) studies. Samples were cut from the fractured region of the tensile test specimens and the surface morphology was examined. The samples were mounted on an aluminum stub using double adhesive tape and sputter-coated with silver in an argon-purged chamber evacuated to 500 mTorr. The coated samples were examined with an accelerating voltage of 20 kV.

To illustrate the general morphology of HAP in PCL, HAP crystals dispersed in PCL were examined by

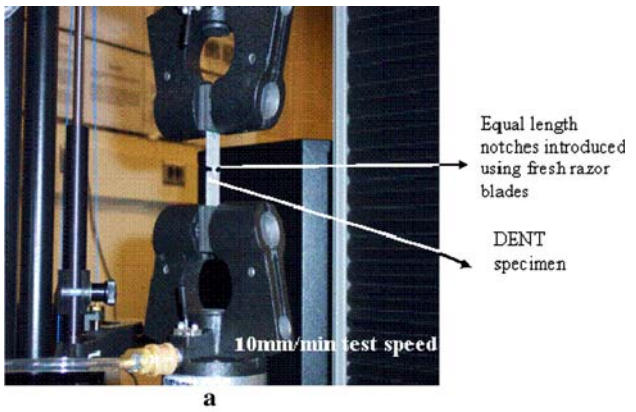

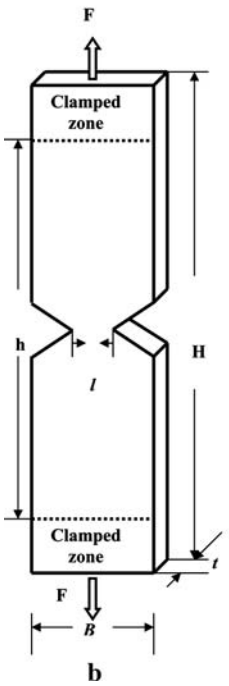

Fig. 2 (**a**) Experimental setup to conduct the EWF tests and (**b**) double-edge-notched-tension (DENT) specimen. H = total length, h = gauge length, l = ligament length, B = specimen width, t = specimen thickness

transmission electron microscopy (TEM). Samples were cut using a Leica Ultracut UCT ultramicrotome. Microtomed thin sections were collected on 200 mesh copper grids and examined by a Philips CM300 TEM at 300 kV in bright field mode.

Results and discussions

Tensile properties

The tensile properties of the biocomposites were determined using the dog-bone specimens. Representative engineering stress-strain curves with varying HAP content

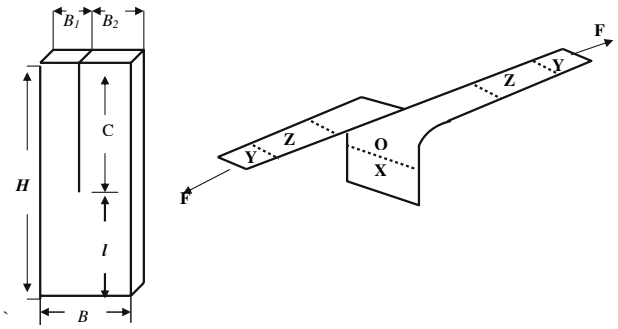

Fig. 3 Schematic of a trousers specimen: The different zones of interest are shown: X represents the region which undergoes tearing; Y is the region where the force is applied; Z is the region subject to uniaxial tension; Region O is present only when the specimen is sufficiently large and when it experiences uniaxial tension; B_1 and B_2 represent the widths of the specimen halves; l is the torn length, C is the pre-notch

are shown in Fig. 4. The tensile modulus for the composites was determined from the initial linear elastic deformation. Generally, the specimens neck and elongate to a significant extent before failure. The peak load at yield and ductility decreased upon the introduction of HAP particles. This finding indicates that the use of HAP in PCL has not been optimized. The presence of HAP filler in the PCL phase appears to create smaller crystallites in semicrystalline PCL, which leads to a reduction in tensile strength [35]. From the ultrastructure of bone it is understood that nanoscale HAP crystals are embedded between the ends of adjoining collagen molecules. The composite of rigid HAP and flexible collagen provides a material that is superior in mechanical properties to either of them alone. Present effort aims to optimize the dispersion of HAP in polymers using high intensity compounding. Plots of Young's

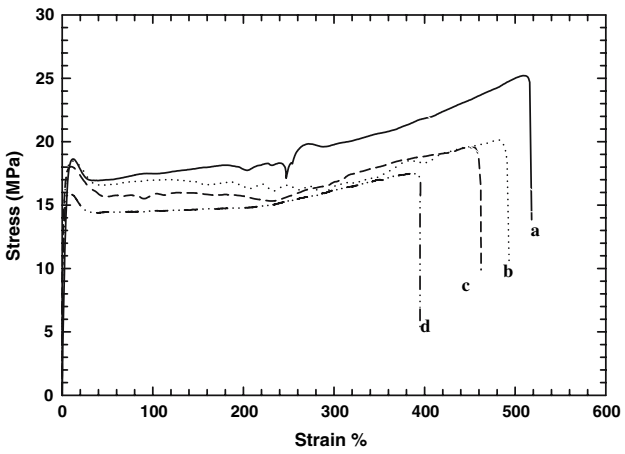

Fig. 4 Representative stress-strain curves for HAP filled PCL: (**a**) 0 wt% HAP; (**b**) 10 wt% HAP; (**c**) 20 wt% HAP: and (**d**) 30 wt% HAP

modulus and tensile strength are shown in Fig. 5 [35]. The results are plotted against the weight fraction of HAP for convenience. Each corresponding volume fraction for 10, 20 and 30 wt% HAP is shown on the top X-axis. The results show significant difference ($p < 0.05$) among the tested composite materials for the mean values of Young's modulus and tensile strength. Addition of HAP increases the modulus slightly, but reduces the tensile strength. Due to the lack of chemical bonds between HAP and PCL, we believe the interfacial stress transfer is controlled by the degree of mixing between the two phases and mechanical interlock [36, 37]. These factors will be considered more independently in our future work.

Fracture properties

The load-displacement curves using DENT specimens for the HAP-filled PCL with different ligament lengths are shown in Fig. 6. Clearly, geometric similarity in loading can be observed. From Fig. 6, the area under the load-displacement curves increases as the ligament length increases. The geometric similarity allows us to deduce that the crack propagates under a consistent fashion and a linear extrapolation to zero ligament length (zero crack growth) gives a physically meaningful fracture parameter, w_e. A fully yielded ligament ensures the inclusion of essential elastic and plastic work, both of which contribute to the FPZ toughness. To verify the tests were performed under fully plane stress conditions, Hill's criterion is invoked [38]. The yield stress was obtained from an average of 5 specimens for each composition. The loading rate used was the same for EWF test. The maximum stress is plotted versus ligament length in Fig. 7. The maximum net section stress for all specimens is found to be less than $1.15\sigma_y$, which satisfies the Hill's criterion. The essential work of fracture is determined from the plot of w_f vs. l using Eq. 2. The specific EWF plots using DENT specimens are shown in Fig. 8. The essential work is derived from a 'best-fit' linear regression analysis of the data. Values of w_e and βw_p were obtained from the y-intercepts and slopes of the linearly extrapolated curves, and the values are given in Table 1 from DENT specimens. w_e decrease as HAP content increases. Pure PCL exhibits the highest w_e value and the values decrease continuously with HAP content. βw_p values decrease as HAP content increases. The values of w_e and w_p obtained by using Eq. 4 are presented in Table 2. As expected, the out-of-plane w_e and w_p values obtained using trousers specimens are lower than those from the DENT specimens. This is commonly observed in semicrystalline polymers and attributed to the molecular orientation and supermolecular arrangement during the tearing process [28].

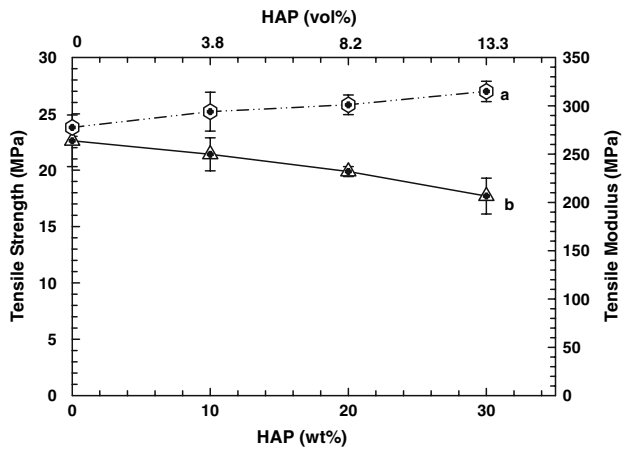

Fig. 5 Young's modulus and tensile strength versus HAP content: (**a**) modulus; and (**b**) yield strength. Note that the corresponding % by volume is indicated on the top X-axis

In addition to PCL, many biodegradable specimens such as polylactic acid and poly(glycolic acid) are characterized by post-yield deformation. Implanted prostheses are often subjected to wear and tear, which induce fracture events. For relatively costly biodegradable samples that exhibit considerable ductility, the EWF and the trousers methods appear particularly beneficial. The EWF technique provides a physically meaningful and reproducible toughness parameter, which can be used for mechanics and structural modeling, under plane stress conditions, which allow thin specimens to be prepared. Extra testing materials can be spared. Mixed-mode fracture behavior [39], which prevails in biological stress states such as in joint spacer, bone cement and other prostheses, can be readily assessed.

Figure 9 shows the TEM micrograph of 20 wt% HAP dispersed in PCL. The HAP particles appear as distinct sub-micrometer scale platelets dispersed in the PCL matrix. The inter-platelet distance is relatively far apart, which suggests constrained reinforcement effect. Figure 10 shows the fractured surface of HAP-filled PCL. The observed surfaces were acquired from the necked regions of tensile specimens. On the fractograph, one can identify HAP particles, which are likely to be derived from the agglomerates of the finer HAP particles that can be seen only under TEM (Fig. 9). The SEM photomicrograph at 10 wt% HAP clearly demonstrates a high degree of localized deformation prior to fracture. From the SEM studies and tensile test data it can be concluded that these biocomposites show extensive ductile deformation, which is constrained upon addition of HAP crystals. The EWF and trousers test methods are of great benefit to characterizing such ductile composites.

The peel strength between adhering layers of HAP and PCL was determined from the peel load-displacement curves. As shown in Fig. 11, the peel force, F, is relatively constant over a considerable distance and gives a value for

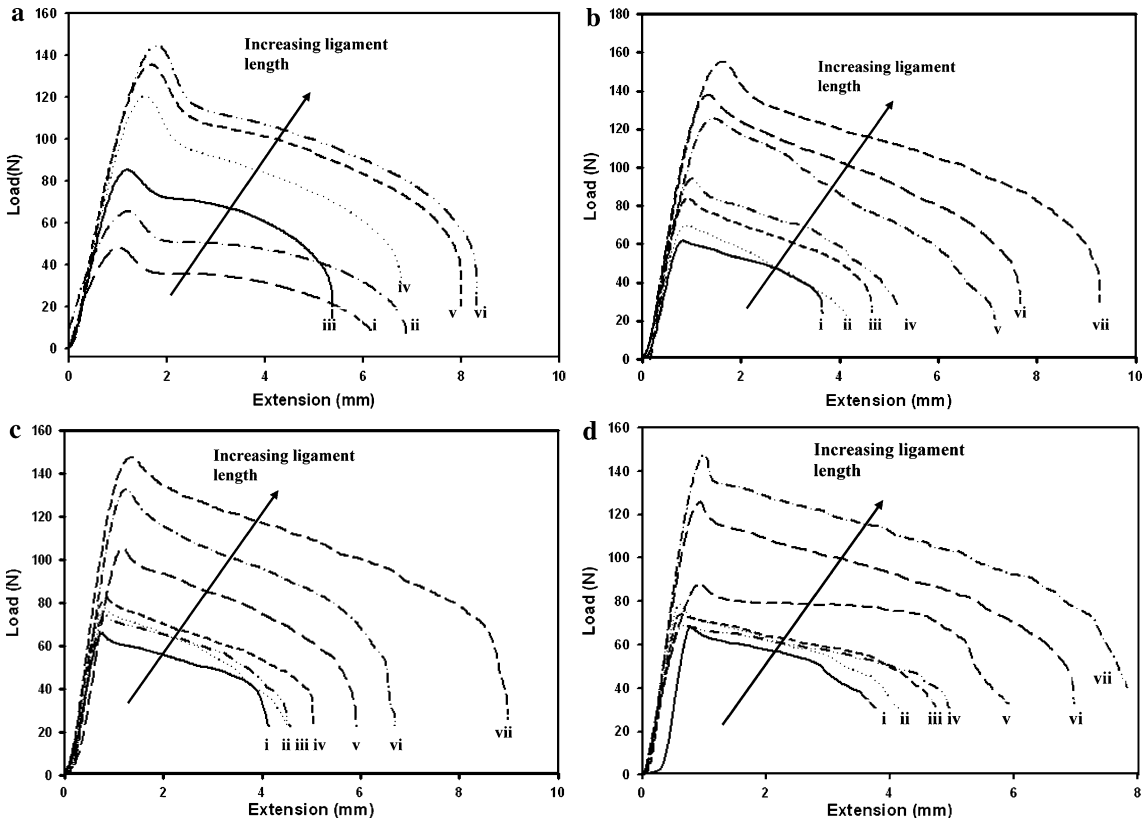

Fig. 6 DENT load-extension curves for HAP filled PCL: (**a**) 0 wt% HAP with ligament lengths: (i) 1 mm; (ii) 2 mm; (iii) 3 mm; (iv) 4 mm; (v) 4.5 mm; and (vi) 5 mm, (**b**) 10 wt% HAP with ligament lengths: (i) 1 mm; (ii) 1.5 mm; (iii) 2 mm; (iv) 3 mm; (v) 3.5 mm; (vi) 4 mm; and (vii) 5 mm, (**c**) 20 wt% HAP with ligament lengths: (i) 1 mm; (ii) 1.5 mm; (iii) 2 mm; (iv) 2.5 mm; (v) 3 mm; (vi) 4 mm; and (vii) 5 mm, (**d**) 30 wt% HAP with ligament lengths: (i) 1 mm; (ii) 1.5 mm; (iii) 2 mm; (iv) 2.5 mm; (v) 3 mm; (vi) 4 mm; and (vii) 5 mm

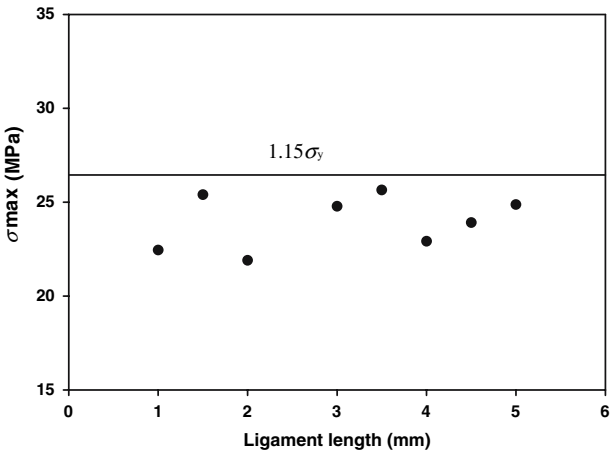

Fig. 7 Plot of net section stress versus ligament length. Horizontal dotted line represents the value of $1.15\sigma_y$ according to the Hill's criterion [38]

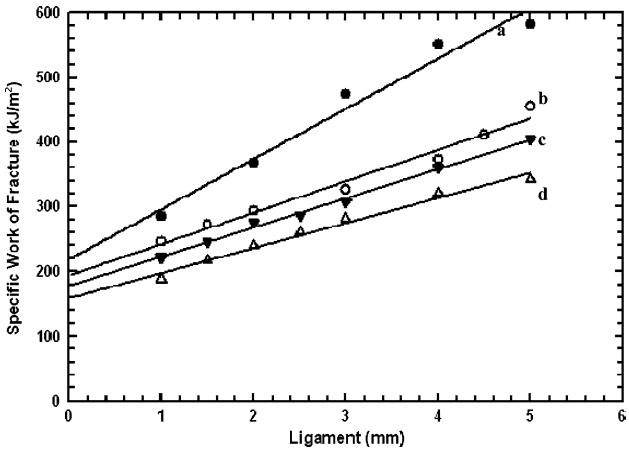

Fig. 8 Specific work of fracture versus ligament length for HAP filled PCL using DENT specimens. (**a**) 0 wt% HAP; (**b**) 10 wt% HAP; (**c**) 20 wt% HAP; and (**d**) 30 wt% HAP. The extrapolated values, w_e, at zero ligament lengths and the linear correlation coefficients, R^2, are provided in Table 1

the fracture energy, $G_A = 2F/t_p$, of the HAP-PCL interface that is relatively high, about 10 kJ/m^2, comparable to that of commercial adhesives. Due to the lack of chemical bonding between HAP and PCL, the adhesive strength measured from peel tests, free of non-essential plastic work, ought to be indicative of the adhesive behavior when

Table 1 Essential work of fracture of HAP-filled PCL from DENT specimens

HAP (wt%)	w_e (KJ/m^2)	βw_p(MJ/m^3)	R^2
0	81.05	4.86	0.986
10	64.26	6.51	0.988
20	62.03	6.56	0.988
30	58.04	6.35	0.965

Table 2 Essential work of fracture of HAP-filled PCL from trousers specimens (w_e and w_p values were determined using Eq. 4)

HAP (wt%)	w_e (KJ/m^2)	w_p(MJ/m^3)
0	75.94	24.03
10	61.53	23.66
20	59.25	21.94
30	57.14	20.40

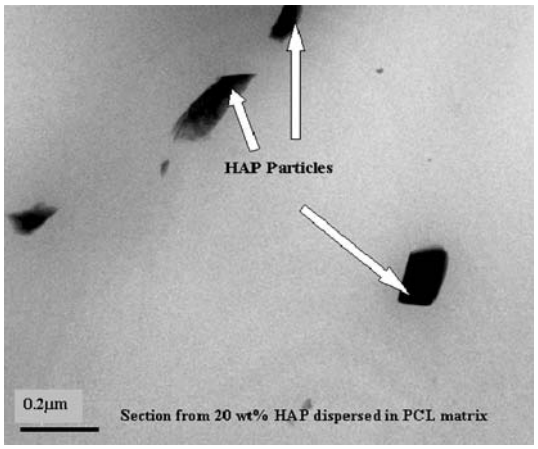

Fig. 9 TEM micrograph of 20 wt% HAP dispersed in PCL

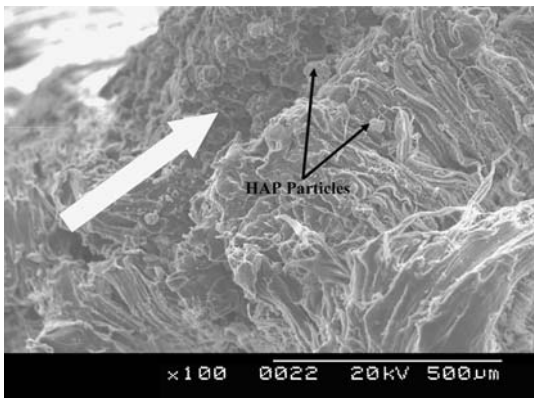

Fig. 10 SEM photomicrograph of the fractured tensile specimen of 10 wt% HAP filled PCL. The white arrow indicates the crack propagation direction

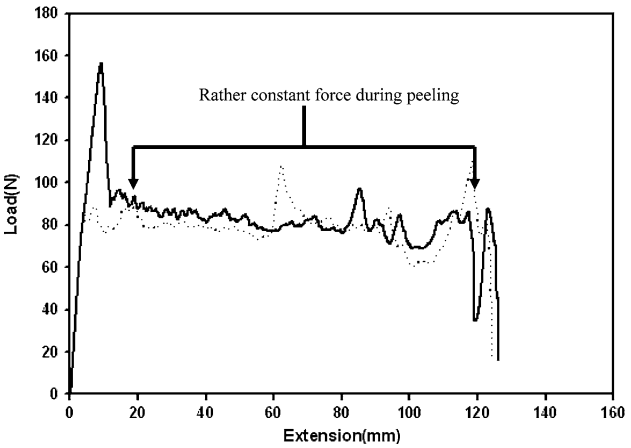

Fig. 11 T-peel load-extension curves for HAP filled PCL

HAP is dispersed in PCL during mechanical mixing such as in an extruder. The specimens were loaded with care to ensure minimal plastic work was operative in peeling. However, the separate contributions of plastic work and interfacial fracture work remain to be determined. Our future work will attempt to eliminate the plastic work from measuring the peel force and the mechanical factors influencing the interfacial work of fracture between HAP and PCL.

Conclusions

Work-of-fracture experiments were conducted to examine the post-yield fracture toughness and interfacial adhesion of a bioactive composite, namely, HAP-filled PCL. It was found that the work of fracture techniques are of considerable value to evaluating the toughness of bioactive composites that exhibit (1) geometric similarity in total fracture work development, (2) post-yield crack propagation, and (3) plane stress fracture due to specimens of reduced thickness. Under such conditions, the EWF approach could provide reliable toughness characterization for analyses and modeling. The tearing specific essential work and the non-essential plastic work of the composites generally decrease as HAP content increases. The decrease was attributed to the change in crystalline morphology of the PCL upon introduction of HAP, which tends to embrittle the intrinsically ductile PCL. Interfacial work of fracture obtained from the T-peel test gave rise to a relatively high value, which indicates the mechanical bonding between the HAP and PCL phases is reasonably strong. The results added promise to using the work of fracture techniques to characterize tearing toughness and interfacial adhesion for bioactive and bone analogue composites.

Acknowledgements One of us (SCW) thanks the University of Akron for the support of a Faculty Research Grant and the National Science Foundation under Award# DMI-0520967. The authors wish to thank Dr. Alan N. Gent for proofreading the manuscript and suggesting future work. His contribution to the interpretation of peel test results and adhesive strength is particularly appreciated.

References

1. J. HAO, M. YUAN and X. DENG, *J. Appl. Polym. Sci.* **86** (2003) 676
2. B. CHEN and K. SUN, *Polym. Test.* **24** (2005) 64
3. M. WANG, *Biomaterials* **24** (2003) 2133
4. M. C. AZEVEDO, R. L. REIS, M. B. CLAASE, D. W. GRIJPMA and J. FEIJEN, *J. Mater. Sci. Mater. Med.* **14** (2003) 103
5. D. W. HUTMACHER, T. SCHANTZ, I. ZEIN, K. W. NG, S. H. TEOH and K. C. TAN, *J Biomed. Mat. Res.* **55** (2001) 203
6. D. W. HUTMACHER, *Biomaterials* **21** (2000) 2529
7. W. SUN, A. DARLING, B. STARLY and J. NAM, *Biotechnol. Appl. Bioc.* **39**, (2004) 29
8. P. QUADRANI, A. PASINI, M. MATTIOLLI-BELMONTE C. ZANNONI, A. TAMPIERI, E. LANDI, F. GIANTOMASSI, NATALI, F. CASALI, G. BIAGINI and A. TOMEI-MINARDI, *Med. Biol. Eng. Comp.* **43** (2005) 196
9. W. SUN, B. STARLY, A. DARLING and C. GOMEZ, *Biotechnol. Appl. Bioc.* **39** (2004) 49
10. K. F. LEONG, C. M. CHEAH and C. K. CHUA, *Biomaterials* **24** (2003) 2363
11. J. W. MELVIN, F. G. EVANS, in "Biomaterials Symposium AMD2", edited by Y. C. FUNG, J. A. BRIGHTON (American Society of Mechanical Engineers, New York, 1973)
12. W. BONFIELD, *J. Biomech.* **20** (1987) 1071
13. T. L. NORMAN, S. V. NIVARGIKAR and D. B. BURR, *J. Biomech.* **3** (1995) 309
14. R. K. NALLA, J. J. KRUZIC, J. H. KINNEY and R. O. RITCHIE, *Biomaterials* **26** (2005) 217
15. R. K. NALLA, J. S. STOLKEN, J. H. KINNEY and R. O. RITCHIE, *J. Biomech.* **38** (2005) 1517
16. G. PEZZOTTI and S. SAKAKURRA, *J. Biomed. Mater. Res.* **65** (2003) 229
17. Y. KHAN, D. KATTI and C. LAURENCIN, *J. Biomed. Mater. Res.* **69** (2004) 728
18. G. WEI and P. X. MA, *Biomaterials* **25** (2004) 4749
19. M. BORDEN, S. AMIN, M. ATTAWIA and C. LAURENCIN, *Biomaterials.* **24** (2003) 597
20. B. COTTERELL, J. K. REDDEL, *Int. J. Fracture.* **13** (1977) 267
21. A. G. ATKINS and Y. W. MAI (Chichester, Ellis Horwood, 1985) p. 301 (and refs therein)
22. Y. W. MAI and B. COTTERELL, *Int. J. Fracture.* **32** (1986) 105
23. Y. W. MAI and B. COTTERELL, *Eng. Fract. Mech.* **21** (1985) 123
24. Y. W. MAI, S. C. WONG and X. H. CHEN, in "Polymer Blends-Performance, Vol 2" (Wiley, New York, 2000) p. 17
25. S. HASHEMI, *Polym. Engg. Sci.* **20** (2000) 798
26. E. CLUTTON, in "Fracture mechanics testing methods for polymers, adhesives and composites" (Elsevier, 2001) p. 175
27. K. N. SAWYERS and R. S. RIVLIN, *Eng. Fract. Mech.* **6** (1974) 557
28. J. KARGER-KOCSIS and T. CZIGANY, *Polymer* **37** (1996) 2433
29. D. E. MOUZAKIS, M. GAHLEITNER and J. KOCSIS-Kocsis, *J. Appl. Polym. Sci.* **70** (1998) 873
30. A. N. GENT and J. JEONG, *J. Mater. Sci.* **21** (1986) 355
31. A. C. CHANG, S. P. CHUM, A. HILTNER and E. BAER, *Polymer* **43** (2002) 6515
32. A. N. GENT and G. R. HAMED, *Polym. Engg. Sci.* **17** (1977) 462
33. A. J. KINLOCH, C. C. LAU and J. G. WILLIAMS, *Int. J. Fracture* **66** (1994) 45
34. D. R. MOORE and J. G. WILLIAMS, in "Fracture Mechanics Testing Methods for Polymers, Adhesives and Composites" edited by D. R. Moore, A. Pavan and J. G. Williams (Elsevier, 2001) p. 203
35. A. Baji, S. C. WONG, T. LIU, T. LI and T. S. SRIVATSAN, J. Biomed. Mater. Res. Appl. Biomat (2007) in press
36. T. Q. LI, M. Q. ZHANG and H. M. ZENG, *J. Mater. Sci. Lett.* **19** (2000) 837
37. L.S. SCHADLER, S. C. GIANNARIS and P. M. AJAYAN, *Appl. Phys. Lett.* **73** (1998) 3842
38. R. HILL, *J. Mech. Phys. Solids.* **1** (1952) 19
39. B. COTTERELL, E. LEE and Y. W. MAI, *Int. J. Frac.* **20** (1982) 243